

1 **Title**

2 Consistent scale-dependency of future increases in hourly extreme precipitation in two
3 convection-permitting climate models

4 **Authors**

5 Samuel Helsen¹, Nicole P. M. van Lipzig (1), Matthias Demuzere (1,2,5), Sam Vanden
6 Broucke (1), Steven Caluwaerts (4), Lesley De Cruz (3), Rozemien De Troch (3), Rafiq
7 Hamdi (3), Piet Termonia (3), Bert Van Schaeybroeck (3), Hendrik Wouters (1,2,6)

8 (1) Department Earth and Environmental Sciences, KU Leuven, Leuven, Belgium

9 (2) Laboratory of Hydrology and Water Management, Ghent University, Ghent, Belgium

10 (3) Royal Meteorological Institute, Belgium

11 (4) Department of Physics and Astronomy, Ghent University, Belgium

12 (5) Department of Geography, University of Bochum, Germany

13 (6) Flemish Institute for Technological Research (VITO), Mol, Belgium

14 **Key Words**

15 CORDEX.be, convection-permitting simulations, COSMO-CLM, ALARO-0, extreme hourly
16 precipitation, climate change, parameterization

17 **Abstract**

18 Convection-permitting models (CPMs) have been proven successful in simulating extreme
19 precipitation statistics. However, when such models are used to study climate change,
20 contrasting sensitivities with respect to resolution (CPM vs. models with parameterized
21 convection) are found for different parts of the world. In this study, we explore to which extent
22 this contrasting sensitivity is due to the specific characteristics of the model or due to the
23 characteristics of the region. Therefore, we examine the results of 360 years of climate model
24 data from two different climate models (COSMO-CLM driven by EC-EARTH and ALARO-0
25 driven by CNRM ARPEGE) both at convection-permitting scale (CPS, ~ 3 km resolution) and
26 non-convection-permitting scale (non-CPS, 12.5 km resolution) over two distinct regions

¹ KU Leuven, Department Earth and Environmental Sciences, Division Geography and
Tourism, Celestijnenlaan 200E, 3001 Leuven

e-mail: samuel.helsen@kuleuven.be

phone: 0497/77.44.32

27 (flatland vs. hilly region) in Belgium. We found that both models show an overall consistent
28 scale-dependency of the future increase in hourly extreme precipitation for day-time. More
29 specifically, both models yield a larger discrepancy in the day-time climate change signal between
30 CPS and non-CPS for extreme precipitation over flatland (Flanders) than for orographically induced
31 extreme precipitation (Ardennes). This result is interesting, since both RCMs are very different
32 (e.g. in terms of model physics and driving GCM) and use very different ways to represent
33 deep convection processes. Despite those model differences, the scale-dependency of
34 projected precipitation extremes is surprisingly similar in both models, suggesting that the this
35 scale-dependency is more dependent on the characteristics of the region, than on the model
36 used.

37

38 **1 Introduction**

39 One of the most severe consequences of climate change is the shift in intensity and frequency
40 of extreme weather events (IPCC, 2013). Changes in extreme and intense precipitation are of
41 particular concern, since they can have large impacts on society through the generation of
42 floods, causing infrastructural damage and even human casualties.

43 Future projections of climate change impacts on extreme precipitation often rely on results
44 obtained by General Circulation Models (GCMs), but the resolution of such models is too
45 coarse to represent extreme precipitation events well (e.g. Tabari et al., 2016). Simultaneously,
46 there exists a large demand for high-resolution climate information by stakeholders, creating a
47 scale discrepancy between the information provided by GCMs and the information required for
48 adaptation strategies. This scale gap can be overcome using the approach of downscaling
49 based on Regional Climate Models (RCMs) (Wang et al., 2004; Maraun et al., 2010; De Troch,
50 2016; Saeed et al., 2017; Termonia et al., 2018).

51 RCMs have been demonstrated to add value with respect to their coarser resolution
52 counterparts, especially in regions with complex topography (Wang et al., 2004). Owing to their
53 higher resolution, the former models are able to account for more spatial details, such as a
54 more realistic representation of orography and land-sea contrasts (Wang et al., 2004; Maraun
55 et al., 2010; Prein et al., 2015; Saeed et al., 2017). Next to that, they additionally improve the
56 treatment of fine scale physical and dynamical processes (Maraun et al., 2010; Kendon et al.,
57 2012; Prein et al., 2016) and they also have been shown to add value in their representation
58 of precipitation and precipitation extremes (Maraun et al., 2010; Tabari et al., 2016), especially
59 on daily timescales (Kendon et al., 2012; Olsson et al., 2015; Maraun et al., 2010; Vanden
60 Broucke et al., 2018). However, regional climate models at non-convection-permitting scales
61 still show important deficiencies in their representation of precipitation extremes at sub-daily
62 timescales (Maraun et al., 2010; Kendon et al., 2017a; Kendon et al., 2012; Vanden Broucke

63 et al., 2018). The resolution of such climate models is still too coarse to explicitly resolve deep
64 convection and therefore, they have to rely on error-prone convection parameterization
65 schemes (Weisman et al., 1997). Common deficiencies are a misrepresentation of the diurnal
66 cycle of convective precipitation (Kendon et al., 2012, 2014; Prein et al., 2015; Brisson et al.,
67 2016; Maraun et al., 2010), an associated too early onset in convective activity (Fosser et al.,
68 2014; Langhans et al., 2013) and a misrepresentation of hourly precipitation extremes (Prein
69 et al., 2015).

70 Recent advances in high-performance computing power allowed refinement of RCM
71 resolutions beyond the scale of 10 km (Prein et al., 2015). RCMs operating at such high
72 resolutions (Convection-permitting Models (CPMs)) typically have resolutions of less than 4
73 km (Weisman et al., 1997), sufficient to allow for an explicit treatment of deep convection (Prein
74 et al., 2015; De Troch, 2016), and thereby reducing uncertainties due to avoiding error-prone
75 convection parameterization (e.g. Mooney et al., 2017). Recently, a number of studies
76 demonstrated the added value of convection-permitting simulations compared to coarser
77 resolution RCMs, mainly for sub-daily timescales (Prein et al., 2015, 2016; Vanden Broucke et
78 al., 2018, De Troch, 2013, Kendon et al., 2019). The most prevalent improvements are a better
79 representation of the diurnal cycle of convection (Kendon et al., 2012; Ban et al., 2014; Prein
80 et al., 2013; Hohenegger et al., 2008; van Lipzig & Willems, 2015a; Fosser et al., 2014; Prein
81 et al., 2015; Brisson et al., 2016; Langhans et al., 2013), an improved spatial precipitation
82 distribution (Vanden Broucke et al., 2018; Ban et al., 2014; Warrach-Sagi et al., 2013; Prein et
83 al., 2013; Hohenegger et al., 2008; Brisson et al., 2016) a better indication of high intensity
84 summer precipitation events (Kendon et al., 2012; Ban et al., 2014; Prein et al., 2013; Chan et
85 al., 2014b; Fosser et al., 2014; Brisson et al., 2016; Tabari et al., 2016; Vanden Broucke et al.,
86 2018), and an improved representation of surface-atmosphere feedbacks (e.g. Hohenegger et
87 al., 2009; Taylor et al., 2013). Next to that, also the formation of clouds related to different land
88 use characteristics are better represented in CPMs (Vanden Broucke et al., 2017). Most
89 studies also agree on the fact that, especially over mid-latitudes, the added value of CPMs is
90 lower for the winter season than for the summer season (Chan et al., 2013; Fosser et al., 2014,
91 Saeed et al., 2016, Vanden Broucke et al., 2018).

92 Many climate change studies have focussed on extreme precipitation, examining for example
93 how extreme precipitation events may evolve under climate change and whether the projected
94 changes differ between convection-permitting scale (CPS, resolution < 4km with explicitly
95 resolved deep convection) and non-CPS (e.g. Vanden Broucke et al., 2018, Giorgi et al. 2016).
96 Kendon et al. (2017), on the one hand, found that changes in seasonal mean precipitation and
97 changes in precipitation occurrence show agreement between CPS and non-CPS for both the
98 summer and winter season. On the other hand, different changes in intensity and duration as

99 well as of daily extremes are found between CPS and non-CPS. The climate change signals
100 are consistent among different studies in terms of larger increases in the intensity of daily
101 precipitation extremes for CPS, especially during the summer months (Chan et al., 2014a;
102 Ban et al., 2015; Saeed et al., 2017).

103 For hourly rainfall, however, projected changes in extreme precipitation vary widely among
104 different studies and between different regions around the world. Some studies found larger
105 increases for hourly precipitation extremes at CPS (Kendon et al., 2019, 2014; Tabari et al.,
106 2016), while others reported little or no differences between CPS and non-CPS (Chan et al.,
107 2014a; Ban et al., 2015; Fosser et al., 2017). According to Vanden Broucke et al. (2018), such
108 differences could potentially be attributed to differences in topographic complexity of the
109 regions under study. More specifically, for Belgium they found a higher sensitivity of extreme
110 precipitation over flatlands compared to hilly areas. A similar dependency was found by Giorgi
111 et al. (2016) over the Alps, with a different sensitivity of the precipitation extremes between the
112 mountainous regions and the surrounding lower areas. Also in other regions around the world,
113 differences in sensitivities with respect to topography are found (e.g. Prein et al., 2017, Shi et
114 al., 2016, Stratton et al., 2018, Kendon et al., 2019), but sometimes with opposite signs or with
115 no dependency on topography. An example of the former are Stratton et al. (2018) and Kendon
116 et al. (2019) over Africa, and an example of the latter is Revadekar et al. (2011) over India, for
117 which the topographical dependency of the extreme precipitation climate change signal is less
118 clear cut. Moreover, regarding the magnitude of the increase in extreme precipitation not all
119 studies agree.

120 Besides topography and scale, other factors can influence the climate change signal of
121 precipitation extremes as well. Generally, results of (convection-permitting) climate
122 simulations are largely model-dependent as a result of inherent uncertainties related to the
123 modelling process (Coppola et al., 2018, Knutti et al., 2010). For example, differences in
124 parameterization schemes between different climate models may contribute to parametric
125 uncertainties but also differences in model physics or differences related to the driving climate
126 model can result in different outcomes regarding the climate change signal (Knutti et al., 2010).
127 Next to that, internal climate variability is a major additional source of uncertainties (e.g. Deser
128 et al., 2012). CPMs are often not able to sample this uncertainty since they are too
129 computationally expensive to be integrated for extended periods (i.e. hundreds of years).
130 Therefore, it is important to consider such factors that may contribute to many uncertainties in
131 the climate change signal of the extremes.

132 The aim of this paper is to explore whether sub-daily extreme precipitation signals differ
133 between different regional climate models. More specifically, we want to examine to which

134 extent the contrasting sensitivities between CPS and non-CPS that are found in previous
135 studies can be attributed to either the specific characteristics of the model (e.g. different ways
136 to simulate deep convection) or to the characteristics of the region (topography). We do this
137 by comparing the output of two different regional climate simulations over a region with a
138 heterogeneous landscape (Belgium), both at CPS (allowing for explicit resolved convection)
139 and non-CPS (deep convection fully parameterized). The corresponding research question
140 that we want to answer in this study is: “Do sub-daily extreme precipitation signals differ
141 between different regional climate models?” With “extreme precipitation signals” we thereby
142 refer to 1) the dependency of the climate change signal to topography (flatland vs. low
143 mountainrange) and scale (CPS vs. non-CPS) 2) the dependency of the climate change signal
144 to the daily cycle (day vs. night), 3) the dependency of the climate change signal to the extreme
145 precipitation intensity and 4) the difference between extreme and seasonal mean precipitation.
146 For this purpose, we make use of twelve sets of 30-year (in total 360 years of) climate
147 simulations over Belgium from the COordinated Regional climate Downscaling EXperiment
148 (CORDEX.be, more information via Termonia et al. (2018) or via <http://www.euro-cordex.be/>).
149 Extreme hourly precipitation statistics are examined based on two different regional climate
150 models (COSMO and ALARO-0) for two separate regions in Belgium with different surface
151 characteristics (flatland vs. hilly regions) and at two different spatial scales (CPS and non-
152 CPS).

153 The paper is organized as follows: Section 2 provides the information about the climate
154 simulation data and regional climate models that were used in this study, as well as the
155 methodology that was used. The results are described in section 3 and a discussion about all
156 the key-results is provided in section 4. In the last section (5), a general conclusion is
157 formulated.

158 **2 Data and methods**

159 **2.1. Model simulations**

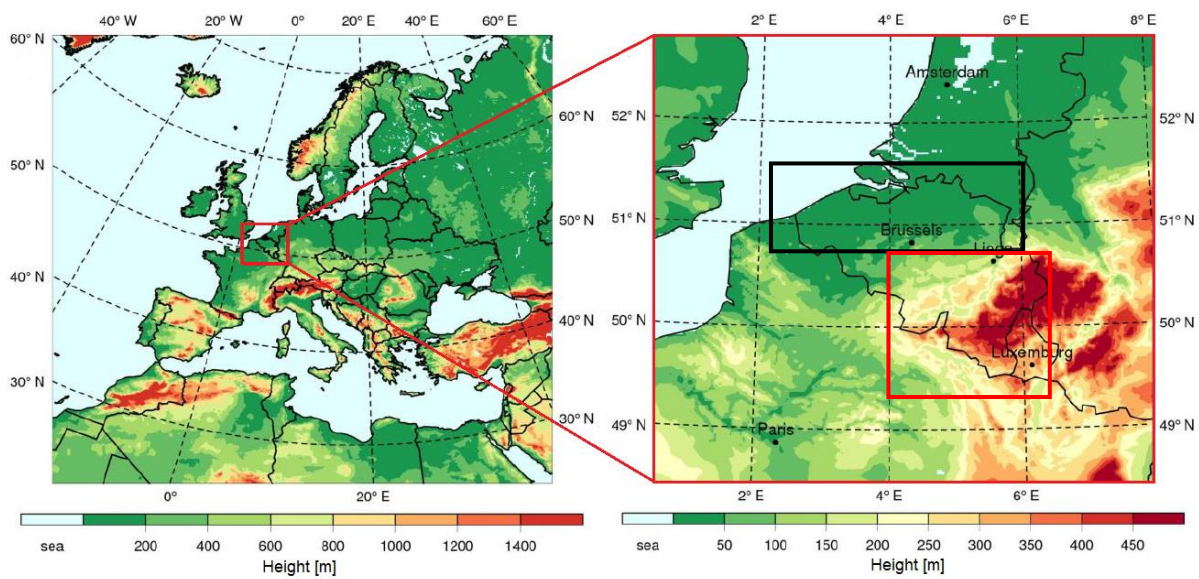
160 Different sets of high-resolution climate model simulations based on two different RCMs
161 (COSMO-CLM and ALARO-0) were used. These model runs were set up by different Belgian
162 research institutions² and were coordinated and provided by the CORDEX.be community. All
163 the CORDEX.be climate simulations were performed using a one-way nesting approach by
164 which both a coarse resolution run (12.5 km) and a high resolution run at convection-permitting

² Katholieke Universiteit Leuven (KUL)

Royal Meteorological Institute of Belgium (RMI)

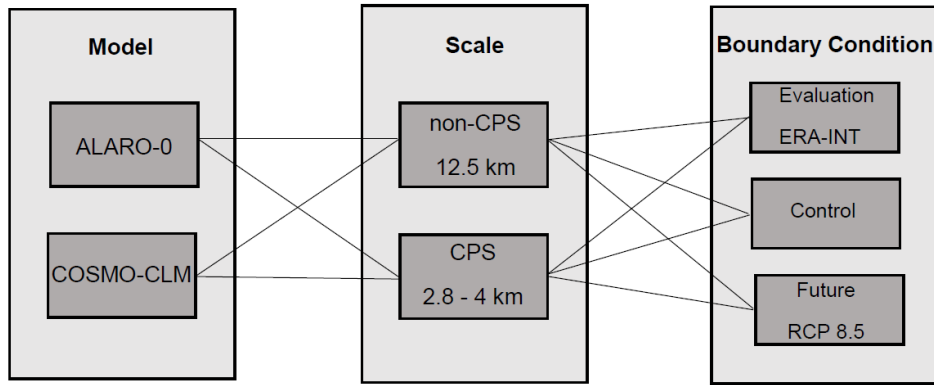
165 scale (CPS, 2-4 km) were provided for each model. In the remainder of this study we will use
166 the term 'CPS' to refer to simulations at convection permitting scale (2.8 or 4 km), while with
167 'CPM' we refer to a convection-permitting regional climate model (ALARO-0 or COSMO-CLM)
168 that is run at CPS with deep convection explicitly resolved, either fully (COSMO-CLM) or
169 partially (ALARO-0).

170 The coarse resolution runs were performed over the EURO-CORDEX domain (Giorgi et al.,
171 2009) at a resolution of 0.11 degrees and the CPS runs were performed over the domain of
172 Belgium with a resolution of 0.035 and 0.025 degrees for the ALARO-0 and COSMO-CLM
173 model, respectively (see fig. 1 and De Troch et al., 2013). Using the one-way nesting strategy,
174 lateral boundary conditions for each of the climate model runs were provided by the coarser
175 resolution model run. For the CPS runs, lateral boundary conditions from the RCM runs were
176 imposed, while for the RCM runs boundary conditions were driven either by a GCM or ERA-
177 Interim re-analysis data (Dee et al., 2011). For each model, three different types of model runs
178 were performed: an evaluation run, a control run and a future run (fig. 2).



179

180 **Fig. 1: Domain size and topography for the CORDEX.be non-CPS runs (12.5 km resolution) over Europe**
181 **(left) and CPS runs (2.8 or 4 km resolution) over Belgium (right). Figure adapted from Vanden Broucke et**
182 **al. (2018). Flanders is indicated by the black rectangle, the Ardennes by the red rectangle.**



183

184 **Fig. 2: A schematic overview of the climate model simulations from CORDEX.be, used in this paper.**
 185 **Convection-permitting scale is abbreviated with CPS, while non-CPS refers to non-convection-permitting**
 186 **scale. Note that both models differ in scale and the way to represent deep convection.**

187 The evaluation simulations were performed for the historical period of 1979-2010 for both
 188 climate simulations with the COSMO-CLM model and for the period of 1950-2010 and 2000-
 189 2011 for the CPS and non-CPS evaluation simulation with ALARO-0 respectively (table 1).
 190 The control simulations were performed for the historical period of 1975-2005 both at non-CPS
 191 scale and at CPS. Boundary conditions for the CPS runs were provided by different GCMs
 192 from the CMIP5 project (Taylor et al., 2012). In this paper we used the RCP 8.5 scenario (Van
 193 Vuuren et al. 2011; Riahi et al., 2011) in order to make climate projections for the end of this
 194 century (2070-2100).

195 **Table 1: Overview of the used climate model simulations.**

Regional Climate Model	Institution	Simulation ID	Resolution (km)	Time Period	Driving global dataset
COSMO CLM	KUL	EU hindcast	12.5	1979-2010	ERA-INTERIM
		BE hindcast	2.8	1979-2010	ERA-INTERIM
		EU control	12.5	1975-2005	ECEARTH
		BE control	2.8	1975-2005	ECEARTH
		EU future	12.5	2070-2100	ECEARTH RCP 8.5
		BE future	2.8	2070-2100	ECEARTH RCP 8.5
ALARO-0	RMI	EU hindcast	12.5	2000-2011	ERA-INTERIM
		BE hindcast	4	1950-2010	ERA-40/ ERA-INTERIM
		EU control	12.5	1975-2005	CNRM-CM5 ARPEGE
		BE control	4	1975-2005	CNRM-CM5 ARPEGE
		EU future	12.5	2070-2100	CNRM-CM5 RCP 8.5
		BE future	4	2070-2100	CNRM-CM5 RCP 8.5

196

197 **2.2. Model description and setup**

198 **2.2.1. COSMO-CLM³**

199 The regional climate model COSMO (COntortium for Small Scale MOdelling) is a non-
200 hydrostatic model that can be used both for Numerical Weather Prediction (NWP) and in
201 CLimate Mode (CLM) for the purpose of regional climate modelling. This model was originally
202 developed by the German Weather Service (DWD) to be used for NWP purposes and is later
203 adapted to be used for long term climate simulations. The COSMO model is now used and
204 further developed for climate related applications by the CLM-Community, an international
205 network of scientists from different research institutes from all over Europe (Rockel et al.,
206 2008). The model has a non-hydrostatic core for atmospheric dynamics and contains
207 parameterizations for radiative transfer, cloud microphysics, subgrid-scale turbulence and
208 convection, ground heat and water transport and land-atmosphere interactions (Wouters et al.,
209 2016).

210 The COSMO-CLM simulations were performed with version 5.0 of the COSMO CLM model.
211 All simulations were executed using the Runge-Kutta two-level time stepping scheme and the
212 Ritter-Geleyn radiation scheme (Ritter & Geleyn, 1992). Moist convection was parameterized
213 using the Tiedtke scheme (Tiedtke, 1989) in the non-CPS simulations, while at CPS deep
214 convection was resolved explicitly and the deep convection scheme was switched off with only
215 shallow convection parameterized. For cloud micro-physics, the schemes of Doms (2007) and
216 Baldauf-Schultz were used (Doms et al., 2011; Baldauf & Schultz, 2004). The urban land-
217 surface model TERRA_URB (Wouters et al. 2012, 2015, 2016, 2017; Demuzere et al., 2017)
218 was implemented, instead of the TERRA_ML scheme. All simulations were performed with 40
219 vertical layers (between 0 and 25 km height) and with timesteps of 20 and 80 seconds at CPS
220 and non-CPS respectively.

221 Lateral boundary conditions for the COSMO-CLM RCM climate simulations (with an update
222 frequency of 6 hours) were provided by the GCM EC-EARTH (table 1), which is part of the
223 CMIP5 multi-model ensemble used in the AR5 of the IPCC (Cubasch et al., 2013). One of the
224 16 members of the EC-EARTH ensemble was downscaled to provide the lateral boundary
225 conditions for the COSMO-CLM RCM runs. For this purpose, the median member of the
226 ensemble was chosen, which is the first member of the EC-EARTH ensemble (for more
227 information see section 2.1 in Vanden Broucke et al., 2018). For our model setup in the
228 COSMO-CLM simulations, the recommendations from Brisson et al. (2015) were taken into
229 account.

³ More information about COSMO-CLM can be found at www.clm-community.eu

230 **2.2.2. ALARO-0**

231 The ALARO-0 model is a hydrostatic model developed within the ALADIN (Aire Limitée
232 Adaptation Dynamique Développement International) community. It is a model version of the
233 ALADIN model, which is the Limited Area Model (LAM) version of the French global ARPEGE-
234 IFS model (Action de Recherche Petite Echelle Grande Echelle Integrated Forecast System)
235 (Bubnová et al., 1995). The ALARO-0 model was originally developed for the purpose of NWP
236 and runs operationally in the countries of the ALADIN consortium. More recently, this model is
237 also used in the context of regional climate modelling (Termonia et al., 2018; De Troch, 2013).
238 The ALARO-0 model was further developed by the Royal Meteorological Institute of Belgium
239 (RMI).

240 The ALARO-0 simulations were based on the dynamical core of the ALADIN model (Bubnová
241 et al., 1995) but employed different physics routines for radiation, microphysics and
242 convection, cloudiness and turbulence (Giot et al., 2016; De Troch et al., 2013). The ALADIN
243 dynamical core is based on a semi-implicit semi-Lagrangian timestepping scheme permitting
244 timesteps of 300 seconds. For radiation the ARPEGE scheme was used (Ritter & Geleyn,
245 1992) while for convection and microphysics the Modular Multiscale Microphysics and
246 Transport (3MT) package was used in combination with a prognostic-type microphysics
247 scheme (Geleyn et al., 2008). The 3MT package was originally developed by Gerard & Geleyn
248 (2005) and further developed and adapted by Gerard (2007) and Gerard et al. (2009). These
249 new physical parameterization schemes have been specifically designed to be used at
250 resolutions in the so-called “grey zone” of convection (below 10 km and above 500 m) at which
251 convection is partially parameterized and partially resolved. In contrast to COSMO-CLM which
252 switches off convection at CPS, ALARO-0 uses both at CPS and non-CPS the same scale-
253 dependent parameterisation scheme. ALARO-0 furthermore employed a semi-Lagrangian
254 horizontal diffusion scheme (Vana, 2008), a pseudo-prognostic turbulent kinetic energy
255 scheme and the land surface model of Noilhan & Planton (1989). All simulations were
256 performed with 46 vertical levels (from the surface to the 4 Pa level) and with time steps of 300
257 seconds for the non-CPS simulations and 180 seconds for the simulations at CPS. Lateral
258 boundary conditions for ALARO-0 were provided by the GCM NCRM-CM5 ARPEGE (table 1),
259 which is also part of the CMIP5 multi-model ensemble used in the AR5 of the IPCC (Cubasch
260 et al., 2013).

261 Both COSMO-CLM and ALARO-0 have a resolution-dependent topography. As a result of that,
262 the CPS simulations yield a higher degree of topographic detail compared to the coarser non-
263 CPS simulations.

264 **2.3. Climatology of the study regions**

265 We focus our analysis on two separate regions of Belgium: Flanders (northern part, black
266 rectangle in Fig. 1) and the Ardennes (southern part, red rectangle in Fig. 1). Both regions
267 have different characteristics with respect to topography, the degree of urbanisation,
268 population density and climatology. Flanders is a relatively flat region, with generally heights
269 between 0 and 200 metres, while the Ardennes are characterised by a more hilly landscape
270 (low-mountain range) with a maximal height of about 694 metres (Fig. 1). Flanders is densely
271 urbanised and characterized by high population densities, whereas the Ardennes is a sparsely
272 populated, more natural area with large patches of forest on the slopes of the low-mountain
273 ranges. Both regions also differ in their climatology. Mean annual temperatures are about 3
274 degrees lower over the Ardennes compared to Flanders. Due to the orography effect (uplift) in
275 the Ardennes, this region receives annually also more precipitation compared to Flanders.
276 Mean annual precipitation over the Ardennes varies between 800 mm in the north and up to
277 1500 mm over the areas with highest elevation. Annual precipitation in Flanders varies
278 between 750 mm near the coast and 850 mm further inland.

279 **2.4. Methods**

280 A model evaluation of both models (see Supplements) clearly indicates the added value of
281 CPS versus non-CPS, consistent with the existing literature (see introduction). The main focus
282 of this study is on the future climate projections of extreme precipitation. We focus our analysis
283 on two topographically-different regions in Belgium. The northern “Flanders” region comprises
284 Flanders, a small part of the southern Netherlands, parts of the North Sea and a very small
285 part of northern France. The southern “Ardennes” region comprises of a large part of Wallonia,
286 western Luxembourg and a small part of northern France (see fig. 1). Since the added value
287 of CPMs for investigating precipitation changes is largest for summer months (see
288 introduction), we focus our analysis on the summer months (JJA). Next to that, the summer
289 season is also the season with highest convective activity in Belgium, providing an extra
290 motivation to focus our analysis on this season (e.g. Goudenhoofdt et al., 2013). We also make
291 a distinction between day- (12-18 UTC) and night-time (00-06 UTC), in order to test the
292 sensitivity of the extreme precipitation statistics to the time period. During the day, convective
293 activity is largest, while the opposite is true for the night-time period, when you have usually
294 less convection and a dominance of large-scale synoptic systems.

295 For our statistical methodology to analyse rainfall extremes, we used a frequency-based
296 method based on percentile thresholds (see e.g. Vanden Broucke et al. (2018)), focussing on
297 both wet and dry days (as suggested by Schar et al. (2016)). More specifically, for a set of
298 extreme percentile thresholds ranging from the 95th until the 99.995th percentile, the
299 corresponding precipitation intensities (mm/hr) were derived for each model simulation and for

300 the observations. For the model evaluation, the frequency of exceedance was determined for
301 each grid-cell out of the subdomain (Flanders & Ardennes), both at CPS and non-CPS and
302 compared the observational precipitation intensities. In order to avoid double-counting of
303 extreme events, a block bootstrapping was applied to the data before calculating the
304 exceedance frequencies. To determine the relative climate change signal, the exceedance
305 frequencies from the control and future simulation were divided and plotted. For these
306 simulations, we calculated the percentile exceedance using the precipitation intensities of the
307 subsequent CPS model simulations of each model. To make a consistent comparison possible
308 between CPS and non-CPS, the CPS data was regridded to the non-CPS grid. The latter does
309 not influence the results much, as comparison between CPS and regridded-CPS were found
310 to be small (Vanden Broucke et al. 2018).

311 As extreme precipitation signals can be highly uncertain due to the often small sample sizes,
312 we performed a bootstrapping on our datasets to provide some uncertainty measures on the
313 extreme precipitation climate change signals. Via a bootstrapping algorithm, we calculated
314 from the original precipitation time series 1000 random resampled time series from which 10
315 percent of the original data was omitted, and calculated the exceedance frequencies and
316 related relative future changes. From this, we obtained a distribution of 1000 possible extreme
317 precipitation exceedance frequencies and their relative future changes, from which we
318 calculated the mean, and the mean signal +/- two standard deviations. This range of two
319 standard deviations around the mean is then plotted on the figures, as a measure of uncertainty
320 for the future change signal. Using a student t-test, the statistical significance of the climate
321 change signal was determined at a significance level of 0.01, in order to determine whether
322 the projected signal differed from the control signal.

323 **3 Results**

324 **3.1. The effect of topography (flat vs. low mountain) and scale (CPS vs. non-CPS)**

325 There is a clear difference between the projected changes of the CPS and non-CPS
326 simulations for the orographically-flat Flanders region during the day (Figs. 3 a & b). At CPS,
327 both models on average project an increase in hourly precipitation extremes during day-time,
328 up to 65% (20-100%) for COSMO-CLM and 80% (35-120%) for ALARO-0. For all CPS
329 simulations, the relative changes in the threshold exceedance increase more for higher
330 precipitation thresholds. The increase in hourly precipitation extremes as seen for the CPS
331 runs is, however, in stark contrast to the non-CPS runs that on average project either small
332 relative changes (ALARO-0) or negative changes (COSMO-CLM) for the day-time period
333 (Figs. 3 a & b). Taking into account the uncertainty ranges around the mean signal, it is

334 apparent that the differences between CPS and non-CPC projections are more outspoken for
335 COSMO-CLM than for ALARO-0.

336 In contrast to the Flanders region, the day-time differences between CPS and non-CPS are
337 much smaller in both models for the hilly area of the Ardennes (Figs 3 c & d). Both CPS and
338 non-CPS project increasing relative changes of day-time extreme hourly precipitation. The
339 increase in the frequency of the hourly extreme precipitation events for the day-time period is
340 also larger for the Ardennes region (60-300% increase) than for Flanders (maximally 120%
341 increase). In the Ardennes, both COSMO-CLM and ALARO-0 simulate an increase in the
342 number of extreme precipitation events over nearly the whole percentile range, while in
343 Flanders the increase is consistent across models for only the upper percentiles.

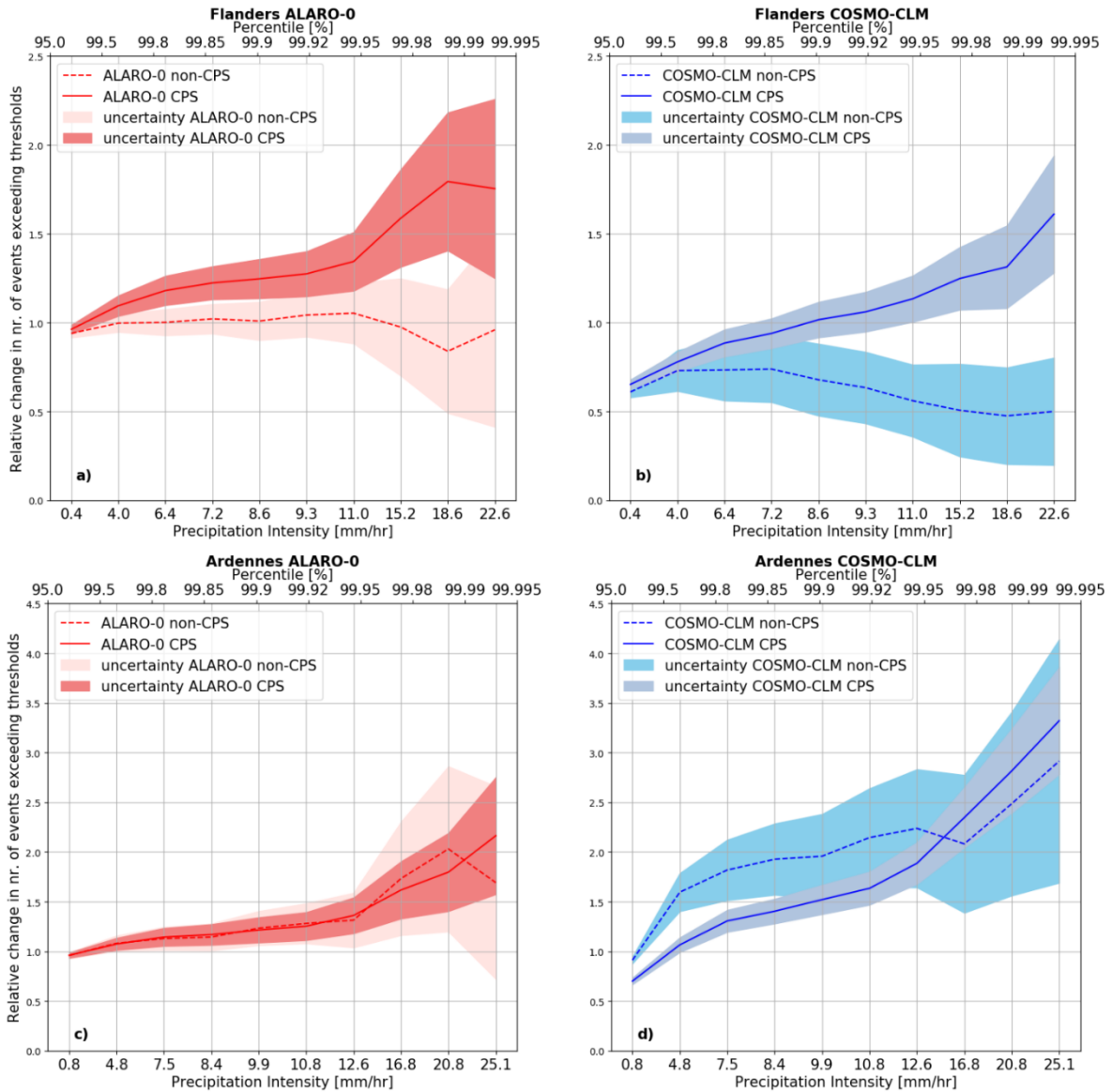


Figure 3: The end-of-the-century (2070-2100) relative change (future/present) in the exceedance frequency of different extreme hourly precipitation intensities during summer (JJA) for Flanders (upper panels, a & b) and the Ardennes (lower panels, c & d) for the day-time period (12-18 UTC). Values higher than one indicate an increase in extremes, while one means no change. Note that the precipitation intensities at the bottom of each figure are the mean of the intensities of all CPMs corresponding to the percentiles indicated at the top of the figure. Note that the scale of the y-axis differs between the upper and lower panels. Note also that all changes were found to be statistically significant, except for P95 of ALARO-0.

344 3.2. Dependency to the daily cycle (day vs. night)

345 There are considerable differences between the extreme hourly precipitation climate change
 346 signals for the day-time (Fig. 3) and night-time (Fig. 4). Both CPS and non-CPS models project
 347 an increase of the night-time extremes for both Flanders and the Ardennes region. In contrast
 348 to the day-time, the COSMO-CLM CPS vs. non-CPS differences are negligible, whereas
 349 ALARO-0 shows different changes between CPS and non-CPS, consistent with the day-time

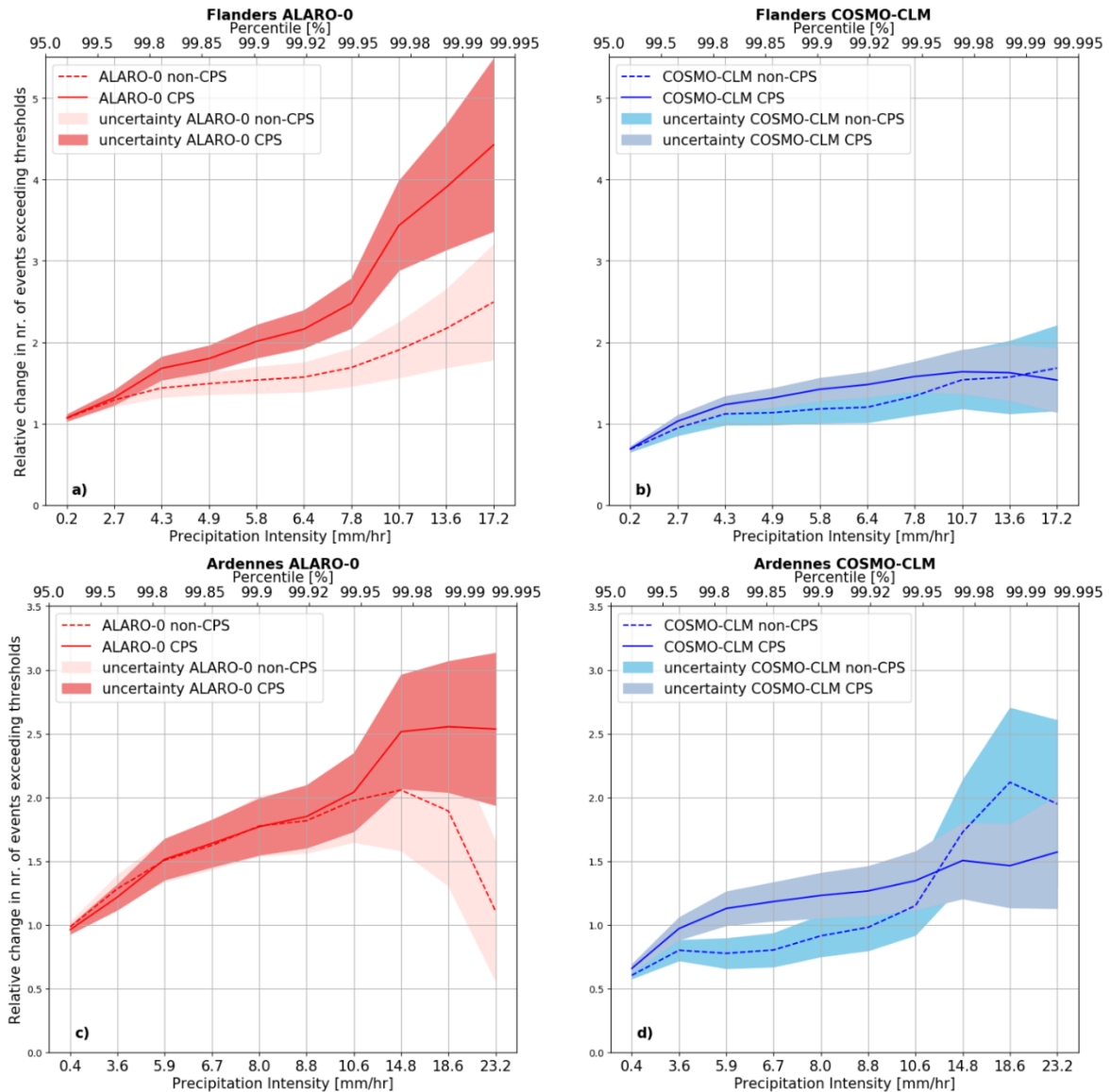


Figure 4: The end-of-the-century (2070-2100) relative change (future/present) in the exceedance frequency of different extreme hourly precipitation intensities during summer (JJA) for Flanders (upper panels, a & b) and the Ardennes (lower panels, c & d) for the night-time period (00-06 UTC). Values higher than one indicate an increase in extremes, while one means no change. Note that the precipitation intensities at the bottom of each figure are the mean of the intensities of all CPMs corresponding to the percentiles indicated at the top of the figure. Note also that the scale of the y-axis differs between the upper and lower panels.

350 signals. For the night-time period, the ALARO-0 CPS simulation also shows a much higher
 351 climate change signal for Flanders (on average up to 350%) compared to the non-CPS (up to
 352 150%) and COSMO-CLM simulations (50-150%). For the Ardennes, the night-time projected
 353 changes in hourly extreme precipitation are very similar at CPS and non-CPS both for
 354 COSMO-CLM and ALARO-0, except for the ALARO-0 highest percentiles.

355

356

357 **3.3. Intensity dependency**

358 The climate change signals also show a clear dependency on the intensities of the extreme
359 precipitation event (or the extreme precipitation percentile) (Figs. 3 and 4). Especially at CPS,
360 the highest increase in the number of extreme precipitation event is expected for the higher-
361 intensity events (upper percentiles). However, since such high-intensity events are extreme
362 and rare, the uncertainty of the climate change signal is also largest for those events with the
363 highest precipitation intensity. The differences between CPS and non-CPS also show a
364 dependency on the intensity, as the difference between both is larger for the higher percentiles
365 compared to the lower percentiles (especially for Flanders during day-time).

366 **3.4. Extreme hourly precipitation vs. seasonal average precipitation**

367 Beside the consistent climate change projections for extreme hourly precipitation between
368 COSMO-CLM and ALARO-0, both models show a differential climate change signal for mean
369 summer precipitation (Fig. 5). COSMO-CLM (driven by EC-EARTH) shows an overall drying,
370 while ALARO-0 (driven by CNRM ARPEGE) simulates a slight increase in mean summer
371 precipitation over large parts of the domain, especially over the northern part. Both models
372 show the drying over the southern and south-eastern part of the country. COSMO-CLM and
373 ALARO-0 also project a decrease in the rainy-hour frequency (number of events > 0.01
374 mm/hr), by the end of this century both at CPS and non-CPS (not shown). Although both
375 models project a decrease in the rainy-hour frequency, the magnitude of this decrease
376 considerably varies between COSMO and ALARO-0 with a higher decrease projected by
377 COCMO-CLM, which is in line with the projections of the mean summer precipitation.

378 **4. Discussion**

379 **4.1. The effect of topography (flat vs. low mountain) and scale (CPS vs. non-CPS)**

380 Both COSMO-CLM and ALARO-0 project an increase in the number of extreme hourly
381 precipitation events during day-time at CPS for Flanders, while this increase is not seen at
382 non-CPS, especially for COSMO-CLM. For the Ardennes, the increase in the future events is
383 found both at CPS and non-CPS, consistently for both models. Our results point thus towards
384 a dependency of the climate change signal of the hourly extreme precipitation events on both
385 the resolution (CPS vs. non-CPS) and the regional topographical characteristics (flatland vs.
386 low-mountain range), that is consistent between the two regional climate models. A
387 comparison between the precipitation statistics for Flanders and the Ardennes showed a small

388 positive correlation between both regions. However, as we showed in our analysis, we see a
389 clear difference in the extreme precipitation statistics between both regions, suggesting that
390 their distinct land characteristics (especially orography) are important control parameters
391 modulating the precipitation intensity, frequency and its climate change signal.

392

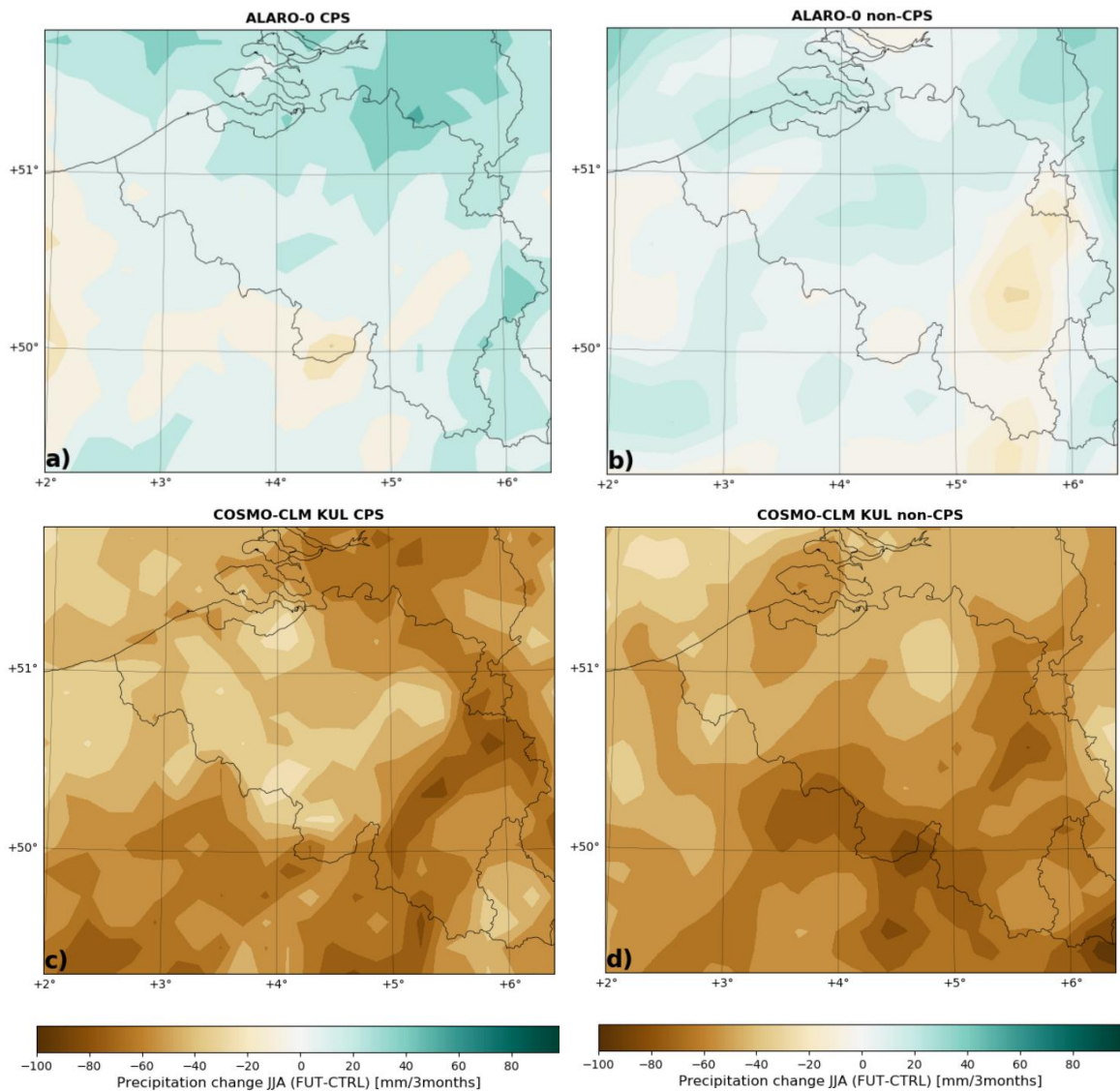


Figure 5: The end-of-the-century (2070-2100) projected change (future-present) in mean summer precipitation (JJA) for Belgium for ALARO-0 (top panels, a & b) and COSMO-CLM ALARO-0 (lower panel, c & d), at CPS (left panels, a & c) and non-CPS (right panels, b & d). The percentiles are calculated on all events over the domain.

393

394 Recently, Vanden Broucke et al. (2018) found a similar topography- and scale dependency of
395 the extreme hourly precipitation over our study domain (Belgium), using only the COSMO-CLM
396 data. Here we found thus that this dependency seems to be independent on the regional
397 climate model that is used, at least for our domain under study. Similar to our findings, Vanden

398 Broucke et al. (2018) also found for COSMO-CLM a higher resolution dependency of the hourly
399 precipitation climate change signal for flatlands (Flanders) compared to hilly areas (Ardennes)
400 and related this topography-scale dependence to the difference in the trigger mechanisms of
401 convection between both types of regions. Extreme precipitation over flatlands such as
402 Flanders is predominantly generated by convection through differential heating over land, a
403 process that is generally not well represented by model simulations using parameterized
404 convection. On the contrary, extreme precipitation over hilly areas is triggered by forced
405 convection over the orography (with orographic uplift), which is taking place at larger scales
406 that can be resolved at coarser scales already, even in models employing parameterized
407 convection. Our study confirms thus the hypothesis of Vanden Broucke et al. that non-CPS
408 simulations are able to capture the day-time increase in hourly precipitation in regions where
409 orography is an important trigger, but not in areas where other processes dominate the
410 triggering of convection and extreme precipitation. However, as discussed in the introduction,
411 studies for other regions around the world point towards diverging conclusions regarding the
412 scale-topography dependency. Since we here only considered two different CPMs and one
413 study region, more similar studies employing other CPMs over other topographically-diverse
414 regions will be needed to generalize our findings.

415 As we found a consistent topography-scale dependency in the day-time hourly extreme
416 precipitation climate change signal for both COSMO-CLM and ALARO-0, our results suggest
417 that the climate change signal for the extremes over our study domain is not sensitive to the
418 way convection is treated in both models. As mentioned in the model description (section 2.2),
419 the ALARO-0 model employs a specific scale-dependent deep convection parameterization
420 scheme (De Troch, 2016; Gerard et al., 2005, 2007, 2009), while deep convection
421 parameterization in COSMO-CLM is scale-independent. More specifically, deep convection
422 parameterization in ALARO-0 is only activated for the scales that cannot be resolved by the
423 grid. In the case of COSMO-CLM, the deep convective parameterization is fully switched on
424 at non-CPS (and fully switched off at CPS). Those differences in parameterization mechanisms
425 result in differences in the performance of both models between CPS and non-CPS for the
426 present-day climate (Supplementary material figs. S2 and S3), with similar results at CPS and
427 non-CPS for ALARO-0 and scale-divergence for COSMO-CLM. The latter is supported by Gao
428 et al. (2017), who also found a reduced sensitivity to the model resolution for a scale-aware
429 regional climate model similar as ALARO-0. As such, the different treatment of deep
430 convection in both models seems to affect the performance of extremes in the present-day
431 climate but does not seem to affect the CPS/non-CPS dependency of the future climate change
432 signal, for which both models show a consistent sensitivity to the model resolution.

433 **4.2. Daily cycle dependency (day vs. night)**

434 For the night-time, when convective activity is generally lower, all simulations project an
435 increase in the number of extreme hourly precipitation events, both for Flanders and the
436 Ardennes. For COSMO-CLM the difference between CPS and non-CPS is much lower than
437 for ALARO-0, especially for Flanders. This seems to suggest that the clear topography-scale
438 dependency, as found for the day-time period, is not valid for the night-time extreme events,
439 that are generally much less frequent and can have other origins than day-time extreme
440 precipitation events. Moreover, ALARO-0 also showed much higher night-time changes for
441 Flanders. We think that this might be related to the higher climate change signal that this model
442 also shows for mean summer precipitation, but more research is needed in order to explore
443 the origin of these high night-time differences more in detail.

444 **4.3. Intensity dependency**

445 Our study points out that the climate change signal of extreme hourly precipitation events is
446 dependent on the precipitation intensity, or the percentile that is considered. We generally find
447 higher future increases in the frequency of the events for the highest-intensity events (upper
448 percentiles). This is in line with Pendergrass (2017), who states that the most extreme events
449 have a different (stronger) response with respect to the climate warming, than the less extreme
450 events. However, they also state that the changes in extreme precipitation statistics depend
451 on the metric that is used. Here we used a frequency-based method based on thresholds and
452 found that the frequency of the highest-intensity events are expected to increase more by the
453 end of this century compared to the less-extreme events (at least for our study domain), this
454 in addition to the increase in intensity that Pendergrass (2017) discusses.

455 **4.4. Extreme hourly precipitation vs. seasonal average precipitation**

456 The magnitude of the climate change signal showed a considerable difference between both
457 models, for extreme hourly precipitation, as well as for mean summer precipitation. The effect
458 of the different driving GCMs behind both RCMs is clearly visible in the climate change signal
459 of mean summer precipitation (Fig. 5). Due to differences between the driving GCMs (ARPEGE
460 vs. EC-EARTH), both RCMs reproduce a different (opposite) change pattern of mean summer
461 precipitation over the study domain. The mean summer precipitation climate change signal is
462 strongly determined by the synoptic forcing prescribed by the Global Circulation Models
463 (GCMs), while the hourly extreme precipitation statistics are influenced by the other factors as
464 well. For example, COSMO-CLM is a non-hydrostatic model, while ALARO-0 is hydrostatic.
465 Next to that, ALARO-0 and COSMO-CLM also differ in their physics and land cover
466 parameters. Moreover, as discussed in section 4.1., also the treatment of deep convection
467 differs between both models. Disentangling the influence of all those different factors on the
468 results is, however, out of the scope of this study.

469 Our results seem to indicate that CPMs produce more robust climate change signals for
470 extreme precipitation (see previous paragraphs) compared to their projected signals for
471 seasonal average precipitation, which are largely driven by the synoptic forcing, induced by
472 their driving GCMs. Although, this is not a particular failing of CPMs, since the non-CPS
473 models show similar large differences at these seasonal scales. This opens opportunities for
474 combining micro-ensembles of just a few CPM members with larger standard RCM ensembles
475 to create scenarios for both seasonal average and extreme precipitation.

476 **5. Conclusions and outlook**

477 Within this paper, summer hourly extreme precipitation events were studied over Belgium
478 using two convection-permitting models (CPMs) from the CORDEX.be initiative (COSMO-CLM
479 and ALARO-0), each spanning a total of 180 years of simulation time. Extreme events were
480 analysed using a threshold-based method based on percentiles for two separate regions with
481 different topography (flatlands vs. hilly region), both at CPS and non-CPS. The research
482 question that we posed was: “Do sub-daily extreme precipitation signals differ between
483 different regional climate models?”. We thereby investigated different “signals” of extreme
484 precipitation such as the differences between CPS and non-CPS in relation to regional
485 differences in topography (flat vs. low mountain), daily cycle differences, dependencies of the
486 climate change signal to the rain intensities and differences between the change signal of
487 extremes and seasonal average precipitation.

488 We found a consistent scale-dependency of the future increase in hourly extreme precipitation
489 for the day-time between both models. For the night-time the scale-dependency was less
490 obvious. For the day-time, COSMO-CLM and ALARO-0 both showed a larger difference in the
491 climate change signal between CPS and non-CPS for extreme precipitation over flatland (Flanders)
492 than for orographically induced extreme precipitation (Ardennes). This result is interesting, since
493 both RCMs are very different (e.g. in terms of model physics land cover parameters and driving
494 GCM) and use very different ways to represent deep convection processes. Despite those
495 model differences, the scale-dependency of projected precipitation extremes is very similar in
496 both models. Our findings therefore suggest that the contrasting scale-dependencies between
497 CPS and non-CPS that were found in previous studies, can be mainly attributed to the
498 characteristics of the region under study (topography and scale) and to a much lesser extent
499 to the specific characteristics of the climate model itself (for example the way deep convective
500 is simulated). However, since other studies in other parts of the world show contrasting results
501 and we only considered two CPMs over one specific region, more similar studies employing
502 other CPMs over topographically-complex regions are needed to generalize our findings. The
503 results also pointed out that the climate change signal is dependent on the rain-intensity that
504 is considered, with generally larger differences between CPS and non-CPS for higher

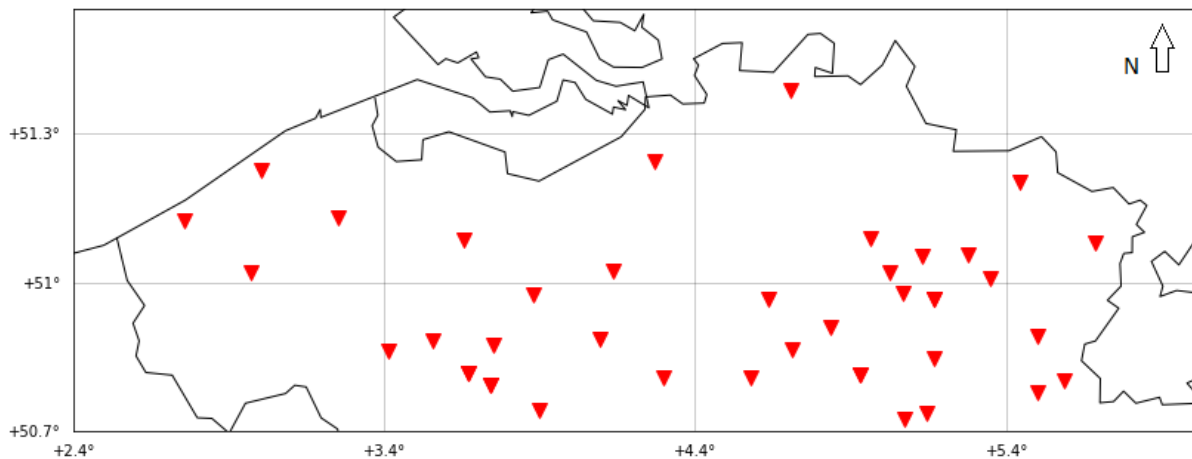
505 intensities and with generally higher increases in the frequency of the extreme events for the
506 highest-intensity events.

507 **Acknowledgements**

508 The work presented here received funding from the Belgian federal government (Belgian
509 Science Policy Office project BR/143/A2/CORDEX.be) and by the European Research Council
510 (ERC), under Grant Agreement No. 715254 (DRY-2-DRY). The computational resources and
511 services used in this work were provided by the VSC (Flemish Supercomputer Center), funded
512 by the Research Foundation –Flanders (FWO) and the Flemish Government—department
513 EWI. The hourly observational data was provided by VMM (Flemish Environmental Agency).
514 These datasets are available at these institutions upon request. The climate model data used
515 in this study can be requested through the CORDEX.be project website (<http://www.euro-corde>
516 [x.be](http://www.euro-corde.x.be)). Finally, we would especially like to thank Erik Van Meijgaard, for providing us with the
517 EC-EARTH GCM data, and for several constructive discussions.

518 **Supplementary Material**

519 For the evaluation part of this study, we employed hourly precipitation observations from 41
520 stations in Flanders (Northern half of Belgium), available for the period 2000-2011 and
521 provided by the Flemish Environmental Agency (VMM). Unfortunately, we did not have access
522 to hourly observations for the Ardennes (Southern half of Belgium).



523

524 **Fig. S1: The 41 hourly observation stations (red triangles) of the VMM, positioned all over Flanders**
525 **(Northern half of Belgium).**

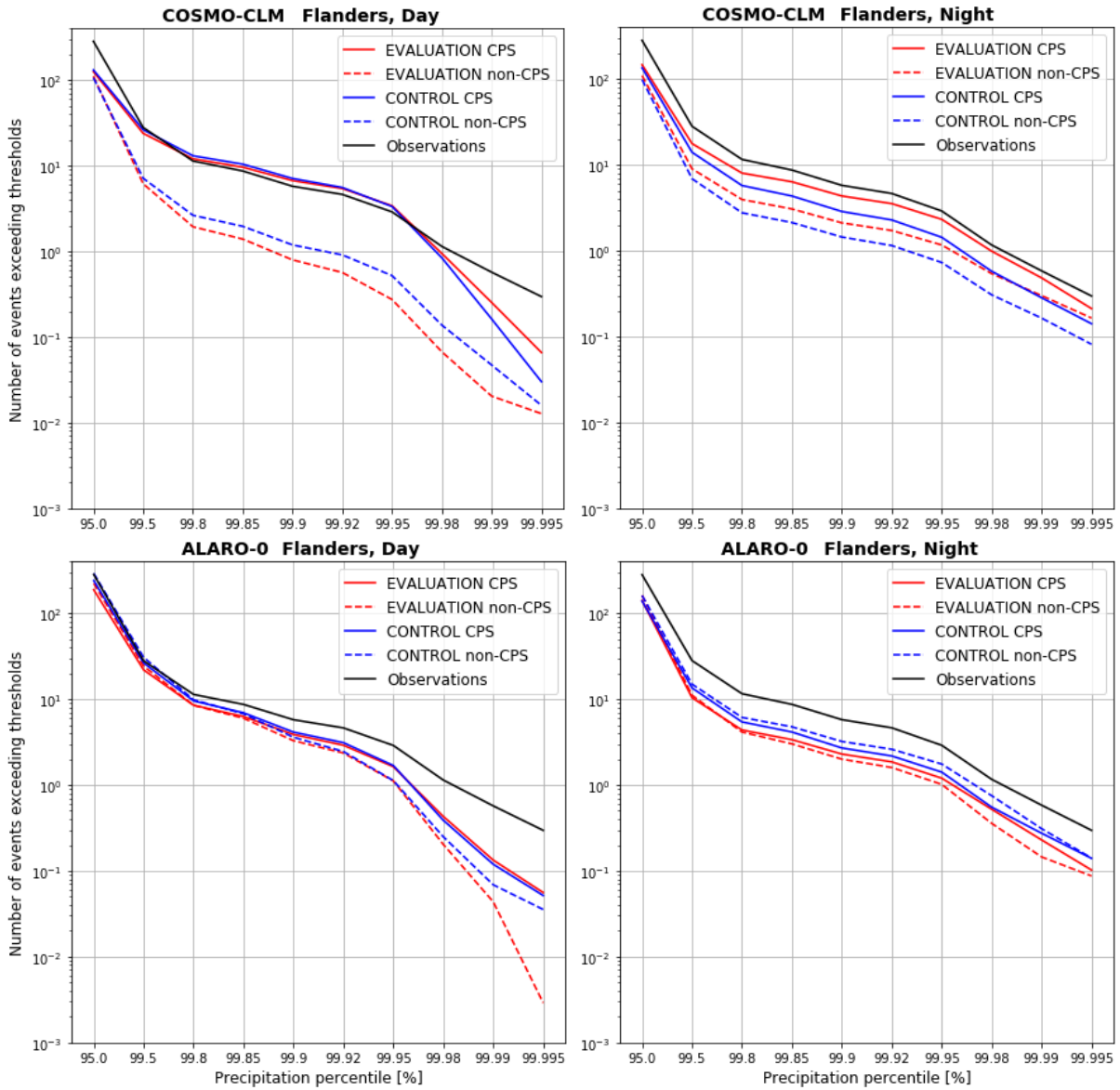


Fig. S2: Present-day summer (JJA) hourly extreme precipitation distributions for Flanders for COSMO-CLM (upper panels) and ALARO-0 (lower panels), for the day-time period (12-18 UTC, left panels) and the night-time period (00-06 UTC, right panels). The distributions are based on the thresholds calculated from the observations. Note that the exceedance numbers (y-axis) are plotted on a logarithmic scale.

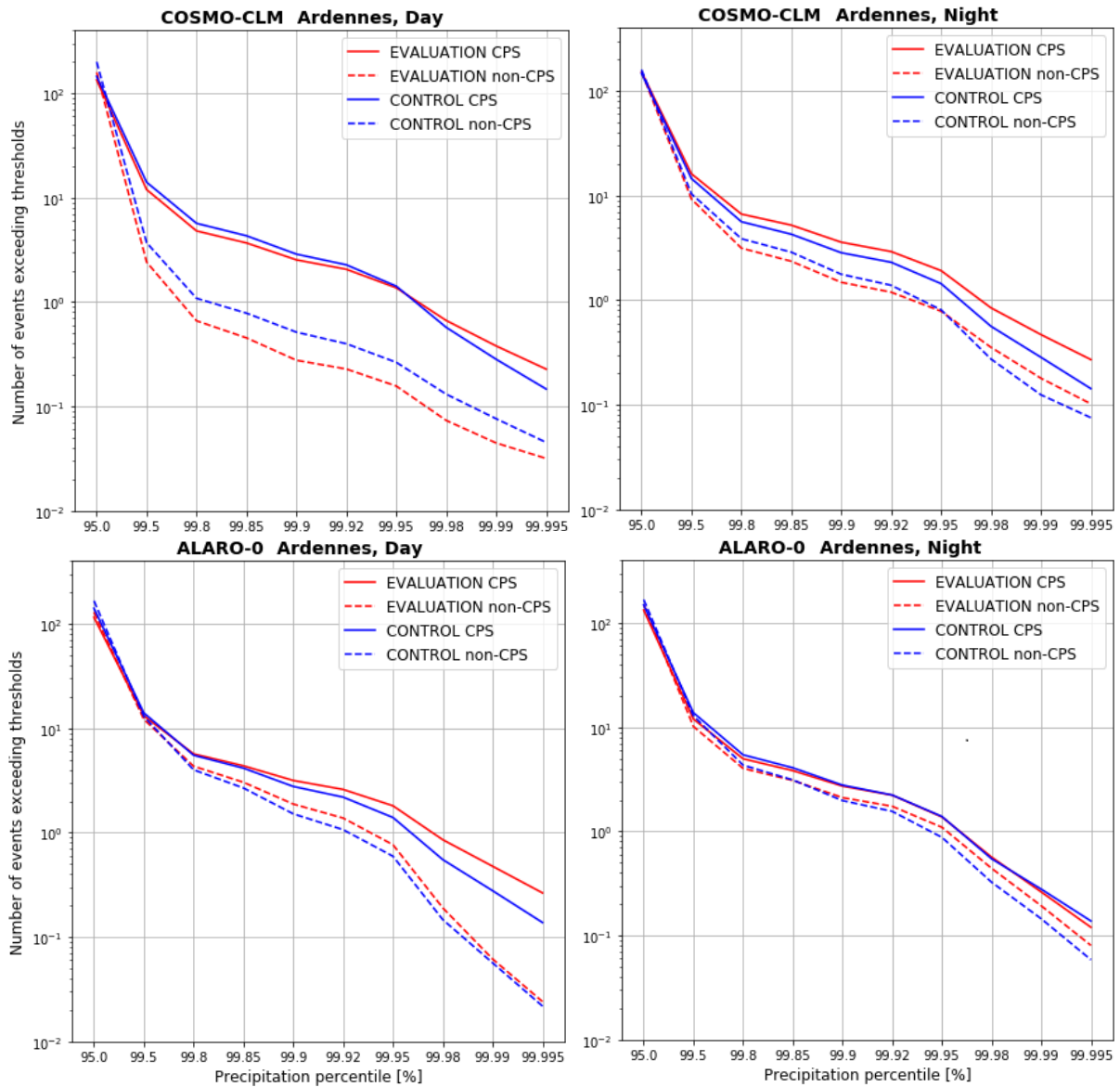


Fig. S3: Present-day summer (JJA) extreme hourly precipitation distributions for the Ardennes for COSMO-CLM (upper panels) and ALARO-0 (lower panels), for the day-time period (12-18 UTC, left panels) and the night-time period (00-06 UTC, right panels). The percentile-thresholds of the CPS simulations were used as reference. Note that the exceedance numbers are plotted on the y-axis on a logarithmic scale.

528 The spatial pattern of the change in the extreme events exceeding the 99.5th percentile differs
 529 considerably between ALARO-0 and COSMO-CLM (Fig. S4). While COSMO-CLM projects a
 530 decrease over large parts of the domain, ALARO-0 projects an overall increase. The difference
 531 between both models is clearly visible on the difference plots (Fig. S5 c & d). The behaviour of
 532 the CPS and non-CPS simulations is similar for both models, which is in accordance with the
 533 analyses in Figs 3 and 4. The differences between CPS and non-CPS is also presented in Fig.
 534 S5 a & b.

535

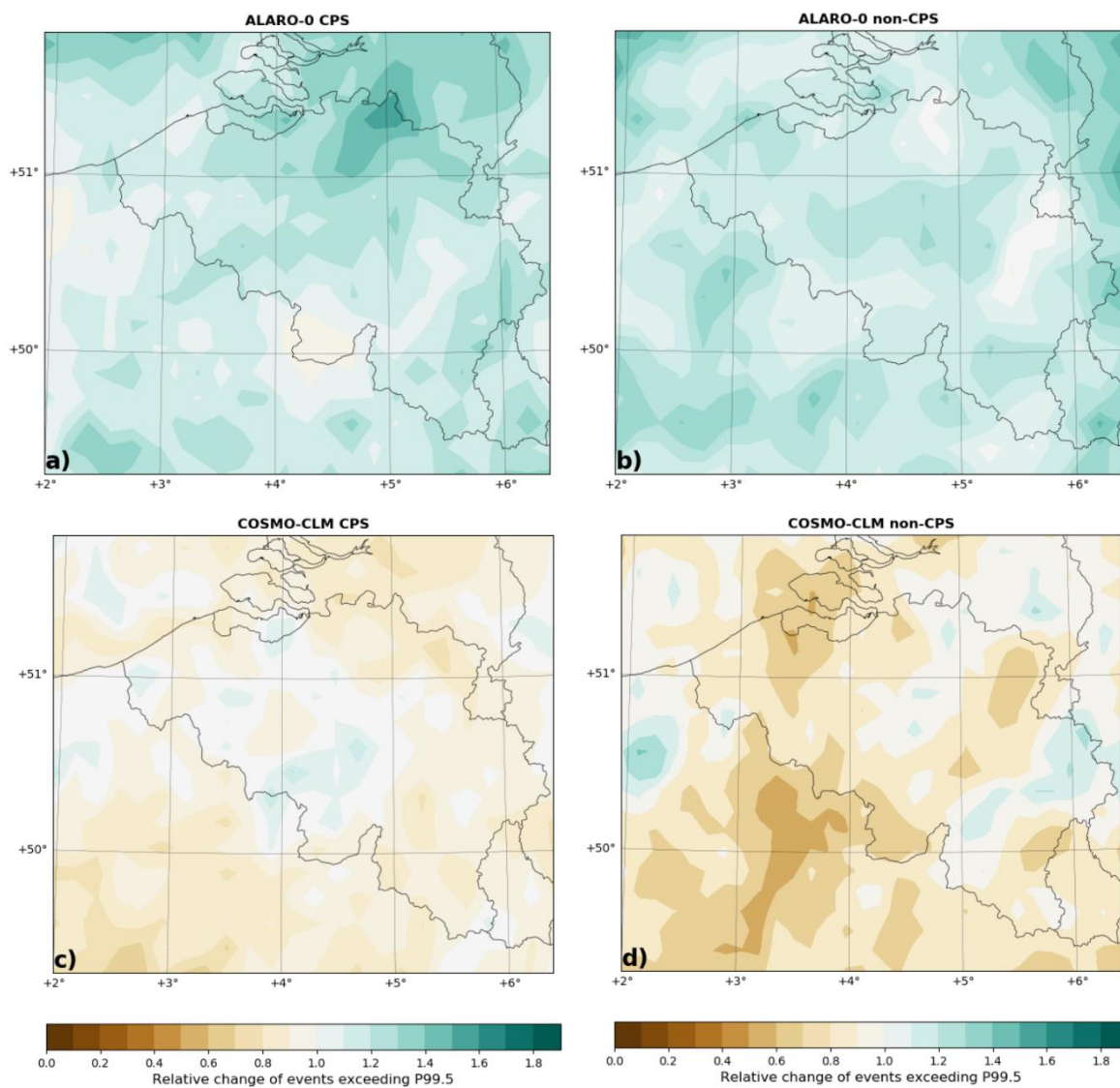


Figure S4: Maps of the end-of-the-century (2070-2100) relative future change (future/present) in the number of events exceeding percentile 99.5 during summer (JJA) for ALARO-0 (top panels, a & b) and 0 COSMO-CLM (lower panels, c & d), at CPS (left panels, a & c) and non-CPS (right panels, b & d). Note that this analysis includes both events during day- (12-18 UTC) and night-time (00-06 UTC).

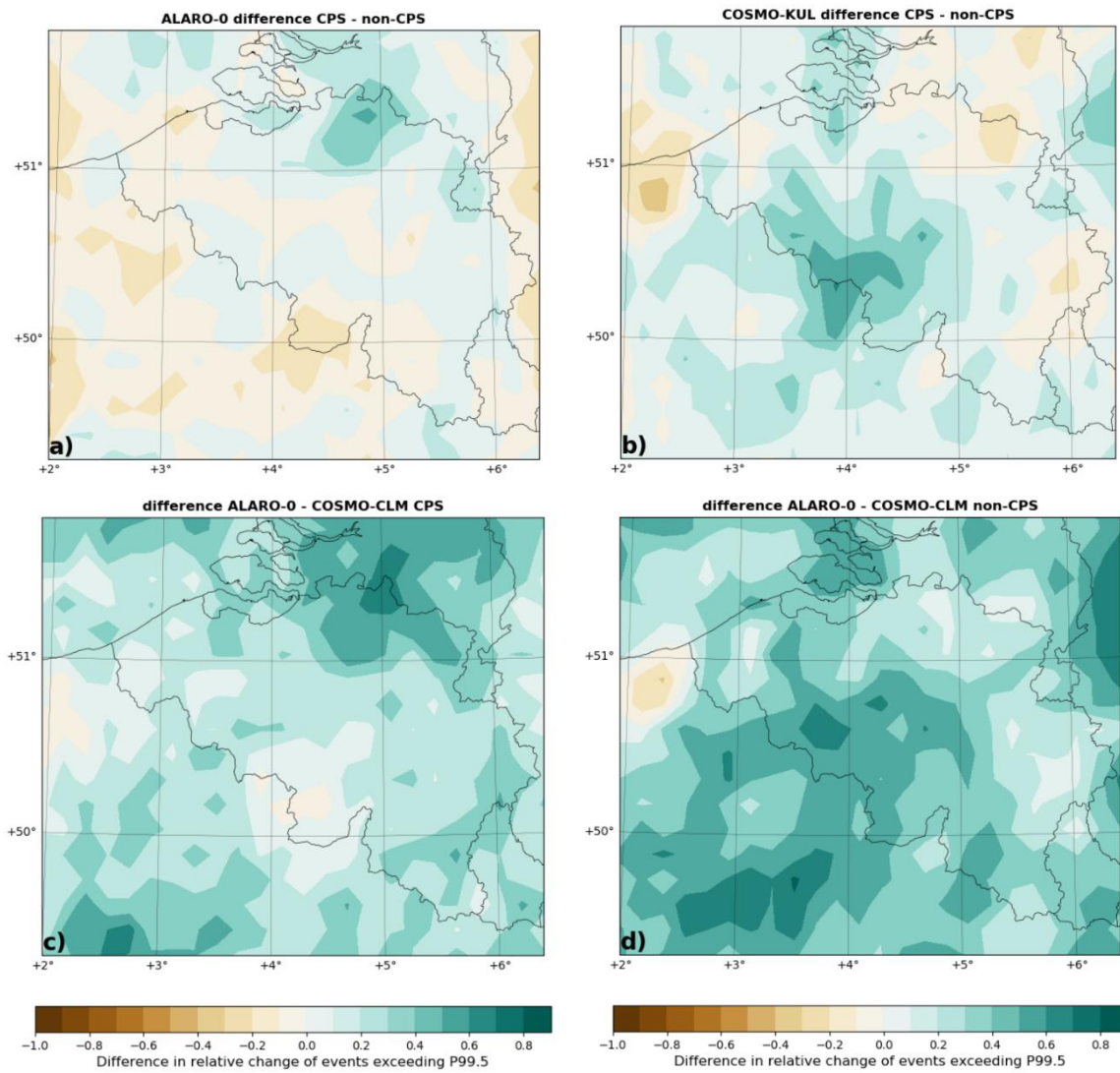


Figure S5: Difference plots between CPS and non-CPS for ALARO-0 (left upper panel, a) and for COSMO-CLM (right upper panel, b) as well as difference plots between ALARO-0 and COSMO-CLM at CPS (lower left panel, c) and at non-CPS (lower right panel, d). The statistic is the change in the number of events exceeding P99.5.

537 **References**

- 538 Ban, N., Schmidli, J. & Schär, C. (2014). Evaluation of the new convective-resolving regional
 539 climate modeling approach in decade-long simulations. *J. Geophys. Res. Atmos.* 119.
 540 p.pp. 7889–7907.
- 541 Ban, N., Schmidli, J. & Schär, C. (2015). Heavy precipitation in a changing climate: Does
 542 short-term summer precipitation increase faster? *Geophysical Research Letters*. 42 (4).
 543 p.pp. 1165–1172.
- 544 Brisson, E., Demuzere, M., Van Lipzig, N. (2015): Modelling strategies for performing
 545 convection-permitting climate simulations. *Meteorologische Zeitschrift*, 25 (2), 149-163.
- 546 Brisson, E., Van Weverberg, K., Demuzere, M., Devis, A., Saeed, S., Stengel, M. & van
 547 Lipzig, N.P.M. (2016). How well can a convection-permitting climate model reproduce
 548 decadal statistics of precipitation, temperature and cloud characteristics? *Climate*
 549 *Dynamics*. 47 (9–10). p.pp. 3043–3061.
- 550 Bubnová, R., Hello, G., Bénard, P. & Geleyn, J.-F. (1995). Integration of the Fully Elastic
 551 Equations Cast in the Hydrostatic Pressure Terrain-Following Coordinate in the
 552 Framework of the ARPEGE/Aladin NWP System. *Monthly Weather Review*. [Online].
 553 123 (2) p.pp. 515–535. Available from:
 554 [http://journals.ametsoc.org/doi/abs/10.1175/1520-](http://journals.ametsoc.org/doi/abs/10.1175/1520-0493%281995%29123%3C0515%3AIOTFEE%3E2.0.CO%3B2)
 555 [0493%281995%29123%3C0515%3AIOTFEE%3E2.0.CO%3B2](http://journals.ametsoc.org/doi/abs/10.1175/1520-0493%281995%29123%3C0515%3AIOTFEE%3E2.0.CO%3B2).
- 556 Chan, S.C., Kendon, E.J., Fowler, H.J., Blenkinsop, S., Ferro, C.A.T. & Stephenson, D.B.
 557 (2013). Does increasing the spatial resolution of a regional climate model improve the
 558 simulated daily precipitation? *Climate Dynamics*. 41 (5–6). p.pp. 1475–1495.
- 559 Chan, S.C., Kendon, E.J., Fowler, H.J., Blenkinsop, S. & Roberts, N.M. (2014a). Projected
 560 increases in summer and winter UK sub-daily precipitation extremes from high-
 561 resolution regional climate models. *Environmental Research Letters*. 9 (8).
- 562 Chan, S.C., Kendon, E.J., Fowler, H.J., Blenkinsop, S., Roberts, N.M. & Ferro, C.A.T.
 563 (2014b). The value of high-resolution Met Office regional climate models in the
 564 simulation of multihourly precipitation extremes. *Journal of Climate*. 27 (16). p.pp. 6155–
 565 6174.
- 566 Coppola, E., Sobolovski, S., Pichelli, E., Raffaele, F., Ahrens, B., Anders, I., Ban, N., Belda,
 567 M., Belusic, D., Caldez-Alvares, A., Cardoso, R. M., Davolio, S., Dobler, A., Fita, L.,
 568 Fumiere, Q., Giorgi, F., Goergen, K., Güttler, I., Halenka, T., Heinzeller, D., Hodnebrog,
 569 Q, Jacob, D., Kartsios, S., Katragkou, E., Kendon, E., Khodayar, S., Kunstmann,
 570 H., Knist, S., Lavín-Gullón, A., Lind, P., Lorenz, T., Marau, D., Marelle, L.,
 571 van Meijgaard, E., Milovac, J., Myhre, G., Panitz, H.-J., Piazza, M., Raffa, M., Raub, T.,
 572 Rockel, B., Schär, C., Sieck, K., Soares, P. M. M., Somot, S., Srncic, L., Stocchi,
 573 P., Tölle, M. H., Truhetz, H., Vautard, R., de Vries, H., Warrach-Sagi, K. (2018). A first-
 574 of-its-kind multi-model convection-permitting ensemble for investigating convective
 575 phenomena over Europe and the Mediterranean. *Climate Dynamics*. p.pp. 1-32.
 576 Available from: <https://doi.org/10.1007/s00382-018-4521-8>.
- 577 Dee, D.P., Uppala, S.M., Simmons, A.J., Berrisford, P., Poli, P., Kobayashi, S., Andrae, U.,
 578 Balmaseda, M.A., Balsamo, G., Bauer, P., Bechtold, P., Beljaars, A.C.M., van de Berg,
 579 L., Bidlot, J., Bormann, N., Delsol, C., Dragani, R., Fuentes, M., Geer, A.J., Haimberger,
 580 L., Healy, S.B., Hersbach, H., Hólm, E. V., Isaksen, I., Kållberg, P., Köhler, M.,
 581 Matricardi, M., McNally, A.P., Monge-Sanz, B.M., Morcrette, J.J., Park, B.K., Peubey, C.,
 582 de Rosnay, P., Tavolato, C., Thépaut, J.N. & Vitart, F. (2011). The ERA-Interim

- 583 reanalysis: Configuration and performance of the data assimilation system. *Quarterly*
584 *Journal of the Royal Meteorological Society*. 137 (656). p.pp. 553–597.
- 585 Deser, C., Phillips, A., Bourdette, V. and Teng, H., 2012. Uncertainty in climate change
586 projections: the role of internal variability. *Climate dynamics*, 38(3-4), pp.527-546.
- 587 De Troch, R. (2016). *The application of the ALARO-0 model for regional climate modeling in*
588 *Belgium : extreme precipitation and unfavorable conditions for the dispersion of air.*
- 589 De Troch, R., Hamdi, R., Van de Vyver, H., Geleyn, J.F. & Termonia, P. (2013). Multiscale
590 performance of the ALARO-0 model for simulating extreme summer precipitation
591 climatology in Belgium. *Journal of Climate*. 26 (22). p.pp. 8895–8915.
- 592 Doms, G., Förstner, J., Heise, E., Herzog, H.-J., Mironov, D., Raschendorfer, M., Reinhardt,
593 T., Ritter, B., Schrodin, R., Schulz, J.-P. & Vogel, G. (2011). Consortium for Small-Scale
594 Modelling A Description of the Nonhydrostatic Regional COSMO Model Part II : Physical
595 Parameterization. *Www.Cosmo-Model.Org*. (September). p.p. 152.
- 596 Fossier, G., Khodayar, S. & Berg, P. (2014). Benefit of convection permitting climate model
597 simulations in the representation of convective precipitation. *Climate Dynamics*. 44 (1–
598 2). p.pp. 45–60.
- 599 Fossier, G., Khodayar, S. & Berg, P. (2017). Climate change in the next 30 years: What can a
600 convection-permitting model tell us that we did not already know? *Climate Dynamics*. 48
601 (5–6). p.pp. 1987–2003.
- 602 Gao, Y., Leung, L., R., Zhao, C., Hagos, S. (2017): Sensitivity of US summer precipitation to
603 model resolution and convective parameterizations across gray zone resolutions.
604 *Journal of Geophysical Research: Atmospheres*. Vol. 122(5), pp. 2714-2733.
- 605 Geleyn, J.F., Catry, B., Bouteloup, Y. & Brožková, R. (2008). A statistical approach for
606 sedimentation inside a microphysical precipitation scheme. *Tellus, Series A: Dynamic*
607 *Meteorology and Oceanography*. 60 A (4). p.pp. 649–662.
- 608 Gerard, L. (2007). On the boundary-layer structure over highly complex terrain: Key findings
609 from MAP. *Quarterly Journal of the Royal Meteorological Society*. 133 (October). p.pp.
610 937–948. Available from: <http://onlinelibrary.wiley.com/doi/10.1002/qj.71/abstract>.
- 611 Gerard, L. & Geleyn, J.F. (2005). Evolution of a subgrid deep convection parametrization in a
612 limited-area model with increasing resolution. *Quarterly Journal of the Royal*
613 *Meteorological Society*. 131 (610 B). p.pp. 2293–2312.
- 614 Gerard, L., Piriou, J.-M., Brožková, R., Geleyn, J.-F. & Banciu, D. (2009). Cloud and
615 Precipitation Parameterization in a Meso-Gamma-Scale Operational Weather Prediction
616 Model. *Monthly Weather Review*. [Online]. 137 (11). p.pp. 3960–3977. Available from:
617 <http://journals.ametsoc.org/doi/abs/10.1175/2009MWR2750.1>.
- 618 Giorgetta, M.A., Jungclaus, J., Reick, C.H., Legutke, S., Bader, J., Böttinger, M., Brovkin, V.,
619 Crueger, T., Esch, M., Fieg, K., Glushak, K., Gayler, V., Haak, H., Hollweg, H.-D., Ilyina,
620 T., Kinne, S., Kornblueh, L., Matei, D., Mauritsen, T., Mikolajewicz, U., Mueller, W.,
621 Notz, D., Pithan, F., Raddatz, T., Rast, S., Redler, R., Roeckner, E., Schmidt, H.,
622 Schnur, R., Segschneider, J., Six, K.D., Stockhause, M., Timmreck, C., Wegner, J.,
623 Widmann, H., Wieners, K.-H., Claussen, M., Marotzke, J. & Stevens, B. (2013). Climate
624 and carbon cycle changes from 1850 to 2100 in MPI-ESM simulations for the Coupled
625 Model Intercomparison Project phase 5. *Journal of Advances in Modeling Earth*
626 *Systems*. [Online]. 5 (3). p.pp. 572–597. Available from:
627 <http://doi.wiley.com/10.1002/jame.20038>.
- 628 Giorgi, F., Jones, C. & Asrar, G. (2009). Addressing climate information needs at the regional

- 629 level: The CORDEX framework. *WMO Bulletin*. 58 (3). p.p. 175.
- 630 Giot, O., Termonia, P., Degrauwe, D., De Troch, R., Caluwaerts, S., Smet, G., Berckmans,
631 J., Deckmyn, A., De Cruz, L., De Meutter, P., Duerinckx, A., Gerard, L., Hamdi, R., Van
632 Den Bergh, J., Van Ginderachter, M. & Van Schaeybroeck, B. (2016). Validation of the
633 ALARO-0 model within the EURO-CORDEX framework. *Geoscientific Model
634 Development*. 9 (3). p.pp. 1143–1152.
- 635 Goudenhoofd E., Delobbe, L. (2013): Statistical characteristics of of convective storms in
636 Belgium derived from volumetric weather radar observations. *J. Appl. Meteorol.
637 Climatol*. 52:918-934.
- 638 Grasselt, R., Schüttemeyer, D., Warrach-Sagi, K., Ament, F. & Simmer, C. (2008). Validation
639 of TERRA-ML with discharge measurements. *Meteorologische Zeitschrift*. 17 (6). p.pp.
640 763–773.
- 641 Hazeleger, W., Severijns, C., Semmler, T et al. (2010): EC-EARTH, a seamless earth-system
642 prediction approach in action. *Bull. Am. Meteorol. Soc*. 91:1357-1363.
- 643 Hazeleger, W., Wang, X., Severijs, C. et al. (2012): EC-EARTH V2.2: description and
644 validation of a new seamless earth system prediction model. *Clim. Dynamics* 39:2611-
645 2629.
- 646 Hohenegger, C., Brockhaus, P. & Schär, C. (2008). Towards climate simulations at cloud-
647 resolving scales. *Meteorologische Zeitschrift*. 17 (4). p.pp. 383–394.
- 648 Hohenegger, C., Brockhaus, P., Bretherton, C.S. and Schär, C., 2009. The soil moisture-
649 precipitation feedback in simulations with explicit and parameterized convection. *Journal
650 of Climate*, 22(19), pp.5003-5020.
- 651 Kendon, E. J., Stratton, R. A., Tucker, S., Marsham, J. H., Berthou, S., Rowell, D. P. and
652 Senior, C. A., (2019). enhanced future changes in wet and dry extremes over Africa at
653 convection-permitting scale. *Nature Communications*. 10. 1794.
- 654 Kendon, E.J., Ban, N., Roberts, N.M., Fowler, H.J., Roberts, M.J., Chan, S.C., Evans, J.P.,
655 Fossier, G. & Wilkinson, J.M. (2017a). Do convection-permitting regional climate models
656 improve projections of future precipitation change? *Bulletin of the American
657 Meteorological Society*. 98 (1). p.pp. 79–93.
- 658 Kendon, E.J., Roberts, N.M., Fowler, H.J., Roberts, M.J., Chan, S.C. & Senior, C.A. (2014).
659 Heavier summer downpours with climate change revealed by weather forecast
660 resolution model. *Nature Climate Change*. 4 (7). p.pp. 570–576.
- 661 Kendon, E.J., Roberts, N.M., Senior, C.A. & Roberts, M.J. (2012). Realism of rainfall in a
662 very high-resolution regional climate model. *Journal of Climate*. 25 (17). p.pp. 5791–
663 5806.
- 664 Langhans, W., Schmidli, J., Fuhrer, O., Bieri, S. & Schar, C. (2013). Long-term simulations of
665 thermally driven flows and orographic convection at convection-parameterizing and
666 cloud-resolving resolutions. *Journal of Applied Meteorology and Climatology*. 52 (6).
667 p.pp. 1490–1510.
- 668 Leutwyler, D., Lüthi, D., Ban, N., Fuhrer, O. & Schär, C. (2017). Evaluation of the convection-
669 resolving climate modeling approach on continental scales. *Journal of Geophysical
670 Research*. 122 (10). p.pp. 5237–5258.
- 671 Maraun, D., Wetterhall, F., Chandler, R.E., Kendon, E.J., Widmann, M., Brienen, S., Rust,
672 H.W., Sauter, T., Themeßl, M., Venema, V.K.C., Chun, K.P., Goodess, C.M., Jones,
673 R.G., Onof, C., Vrac, M. & Thiele-Eich, I. (2010). Precipitation downscaling under

- 674 climate change: Recent developments to bridge the gap between dynamical models
675 and the end user. *Reviews of Geophysics*. 48 (2009RG000314). p.pp. 1–38.
- 676 Mooney, P.A., Broderick, C., Bruyère, C.L., Mulligan, F.J. and Prein, A.F., 2017. Clustering of
677 observed diurnal cycles of precipitation over the United States for evaluation of a WRF
678 multiphysics regional climate ensemble. *Journal of Climate*, 30(22), pp.9267-9286.
- 679 Noilhan, J. & Planton, S. (1989). A Simple Parameterization of Land Surface Processes for
680 Meteorological Models. *Monthly Weather Review*. [Online]. 117 (3) p.pp. 536–549.
681 Available from: <http://journals.ametsoc.org/doi/abs/10.1175/1520-0493%281989%29117%3C0536%3AASPOLS%3E2.0.CO%3B2>.
- 683 Olsson, J., Berg, P. & Kawamura, A. (2015). Impact of RCM Spatial Resolution on the
684 Reproduction of Local, Subdaily Precipitation. *Journal of Hydrometeorology*. [Online]. 16
685 (2). p.pp. 534–547. Available from: <http://journals.ametsoc.org/doi/10.1175/JHM-D-14-0007.1>.
- 687 Pendergrass, A.G., 2018. What precipitation is extreme?. *Science*, 360(6393), pp.1072-
688 1073.
689
- 690 Prein, A.F., Gobiet, A., Suklitsch, M., Truhetz, H., Awan, N.K., Keuler, K. & Georgievski, G.
691 (2013). Added value of convection permitting seasonal simulations. *Climate Dynamics*.
692 41 (9–10). p.pp. 2655–2677.
- 693 Prein, A.F., Gobiet, A., Truhetz, H., Keuler, K., Goergen, K., Teichmann, C., Fox Maule, C.,
694 van Meijgaard, E., Déqué, M., Nikulin, G., Vautard, R., Colette, A., Kjellström, E. &
695 Jacob, D. (2016). Precipitation in the EURO-CORDEX 0.11° and 0.44° simulations: high
696 resolution, high benefits? *Climate Dynamics*. 46 (1–2). p.pp. 383–412.
- 697 Prein, A.F., Langhans, W., Fosser, G., Ferrone, A., Ban, N., Goergen, K., Keller, M., Tölle,
698 M., Gutjahr, O., Feser, F., Brisson, E., Kollet, S., Schmidli, J., Van Lipzig, N.P.M. &
699 Leung, R. (2015). A review on regional convection-permitting climate modeling:
700 Demonstrations, prospects, and challenges. *Reviews of Geophysics*. 53 (2). p.pp. 323–
701 361.
- 702 Revadekar, J.V., Patwardhan, S.K., Rupa Kumar, K. (2011): Characteristic Features of
703 Precipitation Extremes over India in the Warming Scenarios. *Advances in Meteorology*,
704 Vol. 2011 pp. 01-11.
- 705 Riahi, K., Rao, S., Krey, V. et al. *Climatic Change* (2011) 109: 33.
706 <https://doi.org/10.1007/s10584-011-0149-y>
707
- 708 Ritter, B. & Geleyn, J.-F. (1992). A Comprehensive Radiation Scheme for Numerical
709 Weather Prediction Models with Potential Applications in Climate Simulations. *Monthly*
710 *Weather Review*. [Online]. 120 (2) p.pp. 303–325. Available from:
711 <http://journals.ametsoc.org/doi/abs/10.1175/1520-0493%281992%29120%3C0303%3AACRSFN%3E2.0.CO%3B2>.
- 713 Rockel, B., Will, A. & Hense, A. (2008). The regional climate model COSMO-CLM (CCLM).
714 *Meteorologische Zeitschrift*. 17 (4). p.pp. 347–348.
- 715 Saeed, S., Brisson, E., Demuzere, M., Tabari, H., Willems, P. & van Lipzig, N.P.M. (2017).
716 Multidecadal convection permitting climate simulations over Belgium: sensitivity of future
717 precipitation extremes. *Atmospheric Science Letters*. 18 (1). p.pp. 29–36.
- 718 Schär, C., Ban, N., Fischer, E.M., Rajczak, J., Schmidli, J., Frei, C., Giorgi, F., Karl, T.R.,
719 Kendon, E.J., Tank, A.M.K. and O’Gorman, P.A., 2016. Percentile indices for assessing
720 changes in heavy precipitation events. *Climatic Change*, 137(1-2), pp.201-216.

- 721 Schulz, J.P., Vogel, G., Becker, C., Kothe, S., Rummel, U. & Ahrens, B. (2016). Evaluation of
722 the ground heat flux simulated by a multi-layer land surface scheme using high-quality
723 observations at grass land and bare soil. *Meteorologische Zeitschrift*. 25 (5). p.pp. 607–
724 620.
- 725 Stratton, R. A., Senior, C. A., Vosper, S. B., Folwell, S. S., Boutle, J. A., Earnshaw, P. D.,
726 Kendon, E., Lock, A., Malcolm, A., Manners, J., Morcrette, C. J., Short, C., Stirling, A. J.,
727 Taylor, C. M., Tucker, S., Webster, S. and Wilkinson, J. M., 2018. A Pan-African
728 Convection-Permitting regional Climate Simulation with the Met Office Unified Model:
729 CP4-Africa. *Journal of Climate*. 31. p. pp. 3485-3508.
- 730 Tabari, H., De Troch, R., Giot, O., Hamdi, R., Termonia, P., Saeed, S., Brisson, E., Van
731 Lipzig, N. & Willems, P. (2016). Local impact analysis of climate change on precipitation
732 extremes: Are high-resolution climate models needed for realistic simulations?
733 *Hydrology and Earth System Sciences*. 20 (9). p.pp. 3843–3857.
- 734 Taylor, C.M., Birch, C.E., Parker, D.J., Dixon, N., Guichard, F., Nikulin, G. and Lister, G.M.,
735 2013. Modeling soil moisture-precipitation feedback in the Sahel: Importance of spatial
736 scale versus convective parameterization. *Geophysical Research Letters*, 40(23),
737 pp.6213-6218.
- 738 Termonia, P., Van Schaeybroeck, B., De Cruz, L., De Troch, R., Caluwaerts, S., Giot, O.,
739 Hamdi, R., Vannitsem, S., Duchêne, F., Willems, P., Tabari, H., Van Uytven, E.,
740 Hosseinzadehtalaei, P., Van Lipzig, N., Wouters, H., Vanden Broucke, S., van Ypersele,
741 J.P., Marbaix, P., Villanueva-Birriel, C., Fettweis, X., Wyard, C., Scholzen, C.,
742 Doutreloup, S., De Ridder, K., Gobin, A., Lauwaet, D., Stavrakou, T., Bauwens, M.,
743 Müller, J.F., Luyten, P., Ponsar, S., Van den Eynde, D. & Pottiaux, E. (2018). The
744 CORDEX.be initiative as a foundation for climate services in Belgium. *Climate Services*,
745 11 p.pp. 49-61.
- 746 Tiedtke, M. (1989). *Tiedtke Convection Scheme*.
- 747 Vanden Broucke S., Van Lipzig, N. (2017): Do convection-permitting models improve the
748 representation of the impact of LUC? *Climate Dynamics*, 49 (7), 2749-2763.
- 749 Vanden Broucke, S., Wouters, H., Demuzere, M. & Van Lipzig, P.M. N. (2018). The influence
750 of convection-permitting regional climate modeling on future projections of extreme
751 precipitation: dependency on topography and timescale. *Climate Dynamics*.
752 <https://doi.org/10.1007/s00382-018-4454-2>.
- 753 Van Vuuren, D.P., Edmonds, J., Kainuma, M. et al. (2011): The representative concentration
754 pathways: an overview. *Climate Change*, 109:5.
- 755 Van Weverberg, K., Goudenhoofdt, E., Blahak, U., Brisson, E., Demuzere, M., Marbaix, P. &
756 van Ypersele, J.P. (2014). Comparison of one-moment and two-moment bulk
757 microphysics for high-resolution climate simulations of intense precipitation.
758 *Atmospheric Research*. [Online]. 147–148. p.pp. 145–161. Available from:
759 <http://dx.doi.org/10.1016/j.atmosres.2014.05.012>.
- 760 Wang, Y., Leung, L.R., Mcgregor, J.L., Lee, D., Wang, W., Ding, Y. & Kimura, F. (2004).
761 *Regional Climate Modeling : Progress , Challenges , and Prospects*. 82 (January 2004).
762 p.pp. 1599–1628.
- 763 Warrach-Sagi, K., Schwitalla, T., Wulfmeyer, V. & Bauer, H.S. (2013). Evaluation of a climate
764 simulation in Europe based on the WRF-NOAH model system: Precipitation in
765 Germany. *Climate Dynamics*. 41 (3–4). p.pp. 755–774.
- 766 Weisman, M.L., Skamarock, W.C. & Klemp, J.B. (1997). The Resolution Dependence of
767 Explicitly Modeled Convective Systems. *Monthly Weather Review*. [Online]. 125 (4).

- 768 p.pp. 527–548. Available from: <http://journals.ametsoc.org/doi/abs/10.1175/1520->
769 [0493%281997%29125%3C0527%3ATRDOEM%3E2.0.CO%3B2](http://journals.ametsoc.org/doi/abs/10.1175/1520-0493%281997%29125%3C0527%3ATRDOEM%3E2.0.CO%3B2).
- 770 Wouters, H., Demuzere, M., Blahak, U., Fortuniak, K., Maiheu, B., Camps, J., Tielemans, D.
771 & Van Lipzig, N.P.M. (2016). The efficient urban canopy dependency parametrization
772 (SURY) v1.0 for atmospheric modelling: Description and application with the COSMO-
773 CLM model for a Belgian summer. *Geoscientific Model Development*. 9 (9). p.pp. 3027–
774 3054.
- 775 Wouters H., De Ridder K., Van Lipzig N. (2012). Comprehensive Parametrization of Surface-Layer
776 Transfer Coefficients for Use in Atmospheric Numerical Models. *Boundary-Layer Meteorology*,
777 145 (3), 539-550. doi: 10.1007/s10546-012-9744-3
- 778 Wouters, H., Demuzere, M., Ridder, K. De & Van Lipzig, N.P.M. (2015). The impact of
779 impervious water-storage parametrization on urban climate modelling. *Urban Climate*.
780 [Online]. 11 (C). p.pp. 24–50. Available from:
781 <http://dx.doi.org/10.1016/j.uclim.2014.11.005>.
- 782 Wouters H., De Ridder K., Poelmans L., Willems P., Brouwers J., Hosseinzadehtalaei P., Tabari H.,
783 Vanden Broucke S., Van Lipzig N., Demuzere M. (2017). Heat stress increase under climate
784 change twice as large in cities as in rural areas: a study for a densely populated midlatitude
785 maritime region. *Geophysical Research Letters*, 44 (17), 8997-9007. doi:
786 [10.1002/2017GL074889](https://doi.org/10.1002/2017GL074889).
- 787
- 788
- 789